Enhanced Conductivity in Morphologically Controlled Proton Exchange Membranes: Synthesis of Macromonomers by SFRP and Their Incorporation into Graft Polymers

Jianfu Ding,† Carmen Chuy, and Steven Holdcroft*

Department of Chemistry, Simon Fraser University, Burnaby, B.C., V5A 1S6, Canada

Received June 4, 2001; Revised Manuscript Received November 12, 2001

ABSTRACT: A novel series of graft polymers comprising graft chains of a macromonomer poly(sodium styrenesulfonate) (*mac*PSSNa) and a polystyrene (PS) backbone have been prepared using a combination of stable free radical polymerization (SFRP) and emulsion polymerization. Well-defined PSSNa polymers possessing 32 repeat units and a polydispersity index of 1.25 were prepared by SFRP. The pseudo-living chains were terminated with divinylbenzene to afford a macromonomer (*mac*PSSNa), which was subsequently copolymerized with styrene by emulsion polymerization to afford PS-*g*-*mac*PSSNa graft polymers. The number density of macromonomer graft chains was controlled by the feed ratio of macromonomer to styrene. Films were prepared by compression molding and Na^+ ions exchanged for protons to yield proton exchange membranes (PEMs). The graft polymer membranes exhibited lower water uptake but much larger proton conductivity for a given sulfonic acid content compared to membranes prepared from random copolymers of styrenesulfonic acid and styrene (PS-*r*-PSSA). Transmission electron microscopy showed that the graft polymer membranes exhibit a higher degree of phase separation and enhanced connectivity between ionic domains.

Introduction

The proton exchange membrane (PEM) is a key component in solid polymer electrolyte fuel cells. The membrane acts as a separator to prevent mixing of reactant gases and as an electrolyte for transporting protons from the anode to the cathode.[1] Proton conductivity, mechanical strength, and chemical stability of the membrane are major factors that determine fuel cell performance.[2] Nafion is the benchmark PEM, but because of its relatively high cost, effort is focused on the development of alternatives.[3−17]

Many PEMs are based on ionomers that consist of a hydrophobic backbone with pendant cation exchange sites such as SO_3^-. According to the Eisenberg−Hird−Moore (EHM) model,[18,19] the ionic sites aggregate to form multiplets. The size of individual multiplets depends on the ion content and steric constraints.[20] With high ionic content, several multiplets merge to form a continuous ionic phase. The presence of ionic aggregates affects hydration and conductivity of the membrane. High ionic conductivity is observed for Nafion when saturated with ∼31 wt % water.[21,22] Similar effects are found in copolymers of methyl methacrylate and sodium methacrylate for ion contents > 5 mol %.[23] Several models have been proposed to describe the high conductivity of Nafion.[24,25] Gierke proposed a "cluster network" model in which ion clusters, separated by polymer backbone matrix, are connected via short, narrow channels (∼1 nm in diameter).[26] More recent studies indicate that the ionic network is more lamellar-like in nature.[27,28]

Several studies of fuel cell membranes utilize random copolymer or block copolymer ionomers. The latter offer the possibility of further controlling polymer morphology. However, a clear picture of the relationship between structure, morphology, and ion conductivity is yet to be determined, presumably due to the absence of well-defined ionic copolymers with systematically variable structure.

Graft polymers, in which ionic polymer grafts are attached to a hydrophobic backbone, would appear suitable structures for studying structure−property relationships in ion-conducting membranes if the length of the graft and the number density of graft chains can be controlled. In principle, the length of the graft would determine the size of ionic domains, whereas the number density of graft chains would determine the number of ionic domains per unit volume. Collectively, the size and number density of ionic aggregates/clusters are expected to control the degree of connectivity between ionic domains.

In a recent communication, we showed that it is possible to synthesize graft polymers possessing ionic grafts bound to hydrophobic backbones using macromonomers formed by stable free radical polymerization (SFRP) techniques.[29] The polymers are amphiphilic and form ionic aggregates in the solid state. The synthetic aspects of the work made use of recent developments in the SFRP of SSNa,[30,31] the formation of block copolymers of styrene and SSNa,[32] and concepts proposed by Hawker to prepare graft polymers.[31,33] In this paper, we report details on the synthesis and characterization of this novel class of polymer that comprises a styrenic main chain and sodium styrenesulfonate graft chains (PS-*g*-*mac*PSSNa). PS-*g*-*mac*PSSNa was prepared by (1) pseudo-living free radical polymerization of sodium styrenesulfonate (SSNa) and (2) termination with divinylbenzene (DVB). The macromonomer, *mac*PSSNa, serves as both the comonomer and emulsifier in the emulsion copolymerization with styrene. During polymerization, the DVB terminus is located in the core of micellar particles and is incorporated into growing polystyrene (PS) as graft chains. By

* To whom correspondence should be addressed.
† Present address: ICPET NRC, M-12 Montreal Road, Ottawa ON, K1A OR6.

10.1021/ma010970m CCC: $22.00
Published on Web 01/17/2002

Scheme 1. Preparation of PS-*g*-*mac*PSSNa Graft Polymers

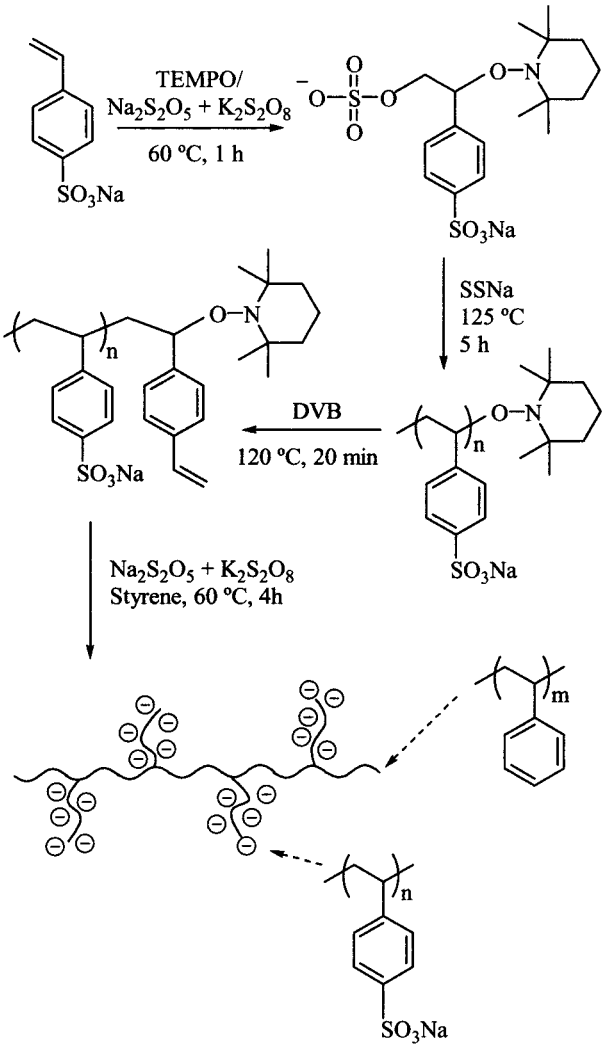

adjusting the *mac*PSSNa/styrene feed ratio, a series of polymers (PS-*g*-*mac*PSSNa) with uniform graft chain length and variable ion content were obtained. For comparison, random copolymers of SSNa and styrene (PS-*r*-SSNa) were prepared by conventional emulsion copolymerization. The two classes of polymer, graft and random, exhibit very different properties of mechanical strength, water uptake, proton conductivity, and thermal behavior as a result of their inherently different morphologies.

Experimental Section

Materials. Sodium styrenesulfonate (SSNa, Aldrich) and 2,2,6,6-tetramethyl-1-piperidinyloxy (TEMPO, Aldrich) were used as received. Styrene and divinylbenzene (DVB, Aldrich 80%) were washed with NaOH solution and H_2O and distilled in the presence of CaH_2 under reduced pressure. Ethylene glycol (EG) was distilled under reduced pressure.

Graft Copolymers of Styrene and Sodium Styrenesulfonate (PS-*g*-*mac*PSSNa). PS-*g*-*mac*PSSNa possessing various sulfonate contents were synthesized in two steps (Scheme 1). SSNa was first polymerized by SFRP in a manner similar to that described by Keoshkerian et al.[30,31] and Bouix et al.[32] A 500 mL round-bottom flask equipped with a reflux condenser was charged with EG (200 mL), SSNa (40.0 g, 194 mmol), and TEMPO (2.960 g, 18.9 mmol). The system was purged with O_2-free N_2. $Na_2S_2O_5$ (1.368 g, 7.2 mmol) in 15 mL of H_2O and $K_2S_2O_8$ (2.592 g, 9.6 mmol) in 45 mL of H_2O were added at 60 °C, and the mixture was stirred for 1 h to form the initiator−TEMPO adduct. The solution was heated to reflux (120−125 °C), and aliquots were removed periodically for analysis of molecular weight. After 5 h, DVB (9 mL, 63 mmol) was added into the solution, and the mixture was refluxed for a further 20 min. The solution was cooled to room temperature, and the polymer was collected by precipitation into an acetone/methanol mixture (60/40 vol). The DVB-terminated PSSNa polymer, *mac*PSSNa, was filtered and dried under vacuum.

*mac*PSSNa (6.0 g) was dissolved in 23 mL of solvent (20 mL of EG/3 mL of H_2O) and the system purged with N_2. 4.0−18.0 mL of styrene was added, the exact amount depending on the desired ratio of styrene to SSNa. The solution was heated to 35 °C, and $Na_2S_2O_5$ (27 mg) in 1.5 mL of H_2O and $K_2S_2O_8$ (42 mg) in 2.5 mL of H_2O were added to initiate polymerization. The solution was stirred for 4 h at 35 °C and 1 h at 50 °C. The polymer was precipitated into 60/40 diethyl ether/methanol, collected by filtration, and air-dried. The crude product was washed with hot water in order to remove polymers containing high *mac*PSSNa content and with THF to similarly remove polymers with low *mac*PSSNa content. The polymer was dried under vacuum.

Random Copolymers of Styrene and Sodium Styrenesulfonate (PS-*r*-SSNa). PS-*r*-PSSNa was prepared by a conventional emulsion copolymerization,[34,35] except that ethylene glycol/water (7:3) was used as solvent. The polymer was washed with H_2O and THF to remove polymers with high SSNa and styrene content, respectively.

Characterization. Molecular weights of PSSNa and *mac*PSSNa were estimated by gel permeation chromatography (GPC, Waters, model M-45) equipped with four Ultrahydrogel columns. The eluant was 0.2 M $NaNO_3$ and 0.01 M Na_2HPO_4 in a mixture of acetonitrile/water (20:80 v/v), and the elution rate was 1 mL/min. The columns were calibrated by PSSNa standards (Polysciences). Compositions of the copolymers were determined with a Bomem 155 FT-IR spectrometer. The relative absorbance of peaks at 1453 and 1010 cm^{-1} (A_{1453}/A_{1010}) were used in the calculation of SSNa content in the polymer, hereafter referred to as ion content (mol %). The ratio of A_{1453}/A_{1010} for different samples was calibrated with values of sulfonate content obtained by elemental analysis (Canadian Microanalytical Service Ltd).[36] Thermal properties were measured with a Perkin-Elmer DSC-7 differential scanning calorimeter under N_2. Measurements of heat flow vs temperature were made in the range 20−300 °C using a heating rate of 20 °C/min. The sample weight was ∼6 mg. T_g and the corresponding difference in heat capacity, ΔC_p, were obtained from the second heating curve.

Membrane Fabrication. Ionomer membranes were prepared by compression molding at 230 °C. Sodium ions were exchanged for protons by immersion in 0.5 M H_2SO_4 for 2 days, followed by rinsing and immersion in deionized water for at least 2 h.

Membrane Thickness, Water Uptake, and Equivalent Weight (EW). The protonated membranes were pat-dried and their weights measured. Thicknesses were measured using a digital micrometer (Mitutoyo). To obtain dry membranes, samples were placed under vacuum at 80 °C and dried to constant weight. The equivalent weight of the membrane was determined by titration. Three samples of each pretreated membrane (acidic form) were individually immersed in 50 mL of 2.0 M NaCl solution for 2 h. Solutions were titrated with 0.025 M NaOH to a phenolphthalein end point. After titration, the sample was rinsed with distilled water and dried under vacuum at 80 °C to constant weight. The equivalent weight was calculated according to eq 1, where W_s is the dry weight (g) of the sample and V_{NaOH} and C_{NaOH} are the volume (L) and molar concentration of NaOH solution, respectively.

$$EW = W_s/(V_{NaOH}C_{NaOH}) \quad (1)$$

Conductivity. A Hewlett-Packard 4194-A impedance analyzer equipped with a 16047 test fixture was used to measure

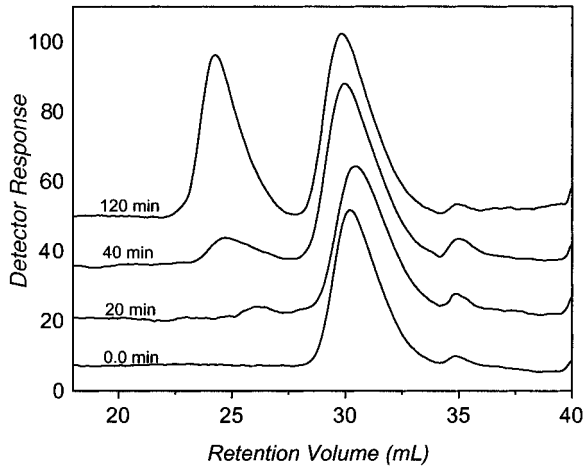

Figure 1. Comparison of GPC traces of PSSNa before and after reaction with DVB.

Table 1. Compositional Data for PS-*g*-*mac*PSSNa

polymer	*mac*PSSNa in feed (mol %)	*mac*PSSNa in copolymer (mol %)	conversion (%)[a] PSSNa	conversion (%)[a] styrene
G10	13.3	10.1	52.2	73.0
G11	16.6	11.9	53.0	79.9
G12	20.1	12.0	49.3	91.7
G13	22.2	13.4	n/a	n/a
G15	23.8	14.8	49.8	90.2
G16	26.6	16.1	50.5	93.7
G19	33.4	19.1	46.6	97.6

[a] Percent conversion of SSNa and styrene monomer into purified graft polymer.

impedance spectra in the frequency range of 100 Hz to 40 MHz. A gold coaxial probe was used as described by Gardner and Anantaraman.[37,38] The accuracy of the measurements was verified by obtaining conductivity values for Nafion 117 (0.05−0.08 S/cm) that are consistent with published results.

TEM. Pretreated membranes (acidic form) were immersed in 2 M $Pb(Ac)_2$ solution overnight and rinsed with water in order to stain the ionic domains. The membranes were dried under vacuum at 80 °C for 8 h, and a 1 × 5 mm strip was cut from the membrane. The sample was sandwiched between two polystyrene films, ~3 mm thick, and hot pressed at 100 °C for 10 min. The sample, fused between PS films, was sectioned along the normal direction to yield 40 nm thick slices using an ultramicrotome (Ultracut-E, Reichert-Jung). The slices were picked up with 600 mesh copper grids for TEM analysis. Micrographs were taken using a Hitachi-7000 microscope operated at 100 kV in the Electron Microscopy Laboratory, Department of Cell Biology and Anatomy University of Calgary.

Results and Discussion

1. DVB-Terminated, Living Free Radical Polymer, Poly(sodium styrenesulfonate) (*mac*PSSNa). To obtain graft polymers with well-defined graft chain lengths, PSSNa was prepared by SFRP. Their molecular weights were controlled by adjusting the ratio of TEMPO to SSNa. The molar ratio of TEMPO to $K_2S_2O_8$ was maintained at 1.97 in order to optimize the reaction. The degree of polymerization, molecular weight, MWD, and conversion of PSSNa were 32, 6.5×10^3 g/mol, 1.25, and 85%, respectively. When the polymerization was complete, DVB was added into the polymerization mixture to afford DVB-terminated PSSNa chains that possess a reactive vinyl group at one terminus. Arguments supporting the successful termination of pseudo-living chains are as follows: It is well-known that styrenic molecules possessing resonance stabilizing

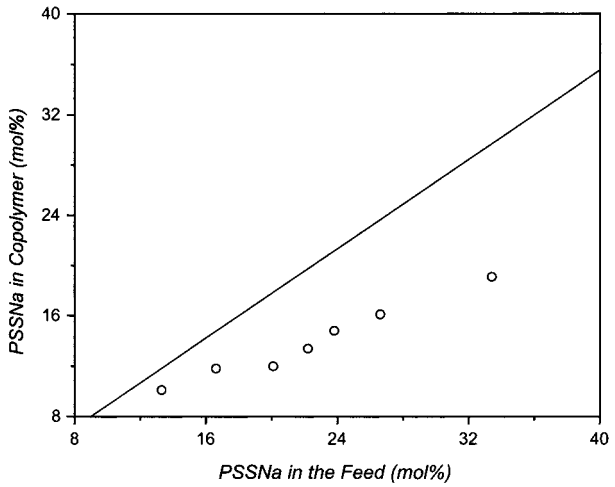

Figure 2. Dependence of the feed composition on the composition of PS-*g*-*mac*PSSNa. Solid line represents theoretical composition.

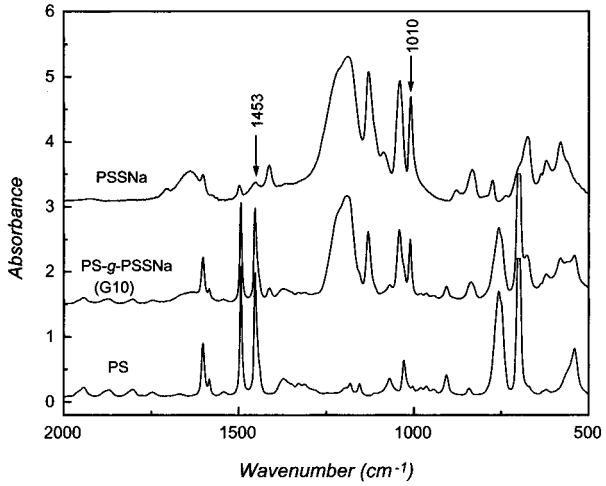

Figure 3. IR spectra of homopolymers of styrene (bottom), sodium styrenesulfonate (top), and PS-*g*-*mac*PSSNa, G10 (middle).

substituents attached to the phenyl ring possess a higher reactivity than unsubstituted styrenes. This is also found to be true in the SFRP of TEMPO-capped substituted styrenics.[31,39,40] It is inferred that TEMPO-capped SSNa radicals react readily with DVB to produce a DVB-terminated living free radical. In the present studies, the molar ratio of DVB to "living" polymer chain was 10:1 in order to ensure capping of all polymer chains. Since a molar excess of DVB was employed, the chain may have continued to propagate by the addition of DVB monomer. However, no increase in molecular weight or polydispersity of PSSNa was evident by GPC analysis when the reaction time was limited to <20 min (Figure 1). Figure 1 shows the emergence of a small, high molecule weight peak (M_n 4.0×10^4) after 20 min reaction time, indicating partial coupling between chains via $-CH{=}CH_2$ terminal groups. With further reaction time, this high molecular weight peak increased in magnitude and shifted to higher molecular weight. The high molecular weight fraction reached 45 wt % of the total polymer sample after 120 min and possessed a M_n of 1.16×10^5. However, when the molecular weight is taken into consideration, the mole fraction of chains possessing the high molecular weight represents only 4% of the total number of polymer chains. When the

Table 2. Characterization of the PS-*g*-*mac*PSSNa(A) and PS-*r*-PSSNa(A) Polymer Membranes

polymer	SS (%)[a]	EW(IR) (g/mol)	EW(Titr) (g/mol)	T_g (°C)[b]	ΔC_p (J/(g K))[b]	H_2O[c] (vol %)	$[H_2O]/[SO_3^-]$[c]	σ[c] (Ω^{-1} cm^{-1})
graft								
G10	10.1	1130	1160	106	0.20	9.9	11.4	0.0069
G11	11.9	980	990	105	0.18	12.8	11.6	0.013
G12	12.0	970	980	106	0.18	9.4	11.7	0.012
G13	13.4	880	830	105	0.15	18.6	15.4	0.045
G15	14.8	800	810	105	0.16	13.5	11.7	0.032
G16	16.1	750	740	104	0.14	21.0	13.3	0.054
G19	19.1	650	640	103	0.12	37.3	17.1	0.24
random								
R10	9.6	1290	1220	110	0.14	12.3	10.1	0.00058
R12	12.0	970	1070	110	0.13	24.2	17.2	0.0023
R17	16.8	720	810	107	0.09	40.5	27.2	0.0041

[a] Determined from FTIR. [b] As Na^+ form. [c] As H^+ form.

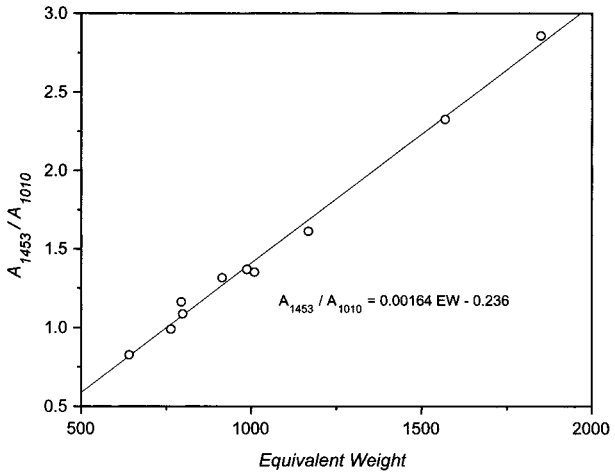

Figure 4. Equivalent weight calibration curve obtained from IR analysis and elemental analysis of PS-*g*-*mac*PSSNa. IR data represent the ratio of absorbances at 1453 and 1010 cm^{-1}.

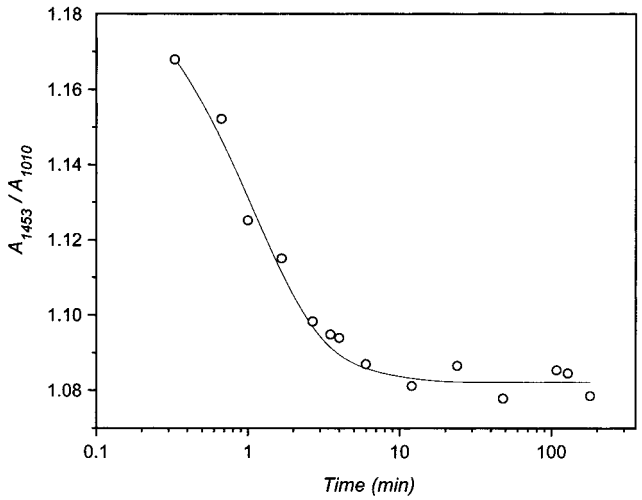

Figure 5. Effect of moisture on the ratio A_{1453}/A_{1010} for a PS-*g*-*mac*PSSNa graft polymer with an ion content of 16.1 mol %.

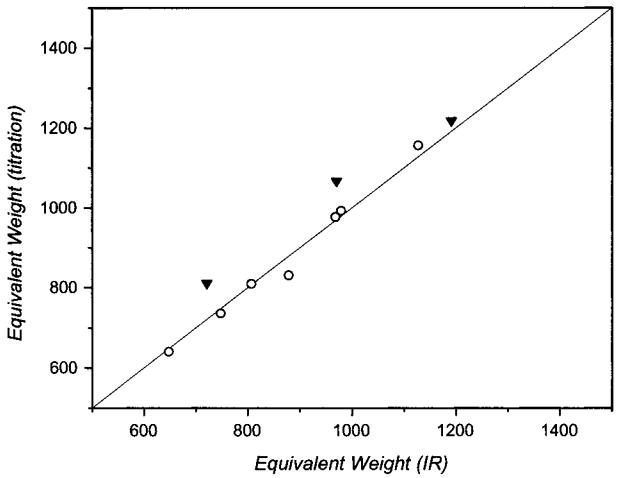

Figure 6. Plot of EW measured by FTIR and by titration: (circle) PS-*g*-*mac*PSSNa, (triangle) PS-*r*-PSSNa.

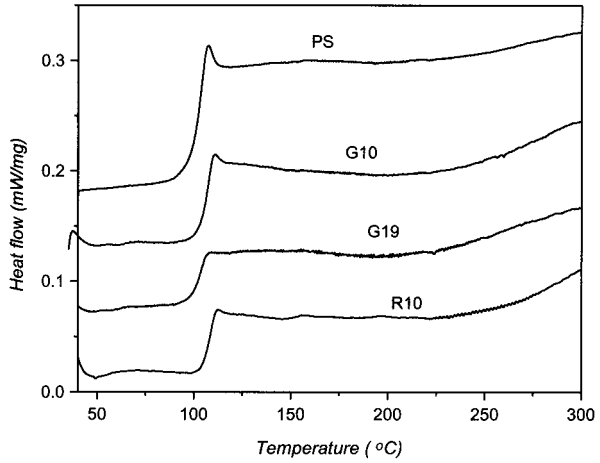

Figure 7. DSC curves of polystyrene (PS), PS-*g*-*mac*PSSNa possessing ion content of 10.1 mol % (G10), and 19.1% (G19), PS-*r*-PSSNa, ion content 9.6% (R10).

reaction time is <20 min, this value is <1%. Thus, to reduce interchain cross-linking, reaction times were kept below 20 min. Under these conditions, the chains possess at least one DVB terminal unit, as evidenced in the next section by the fact that they are incorporated into graft copolymers.

2. Synthesis of PS-*g*-*mac*PSSNa. Styrene was copolymerized with *mac*PSSNa in a heterogeneous styrene/water/EG system. The initial emulsion was poor because the hydrophobic DVB tail of the macromonomer/emulsifier is short. The reaction was initiated by adding the initiator mixture into the solution at 35 °C. Copolymerization of styrene with *mac*PSSNa improved the quality of the emulsion. The terminal vinyl group of *mac*PSSNa is presumed to locate in the hydrophobic core of the particle and due to its close proximity to growing polystyrene chains is statistically incorporated. Table 1 lists the molar percentage of PSSNa in the feed and in the recovered copolymer, together with the percent conversion of styrene into graft polymer.

Under the assumption that styrene and the vinyl group of *mac*PSSNa possess similar reactivity ratios,

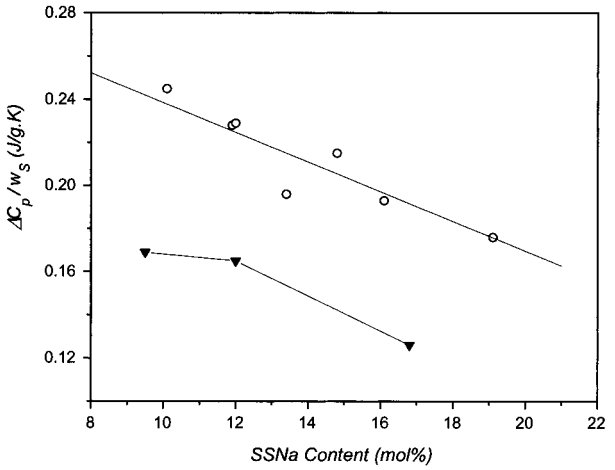

Figure 8. Effect of ion content on the difference in heat capacity associated with T_g and normalized to the mass fraction of PS. (circle) PS-*g*-*mac*PSSNa; (triangle) PS-*r*-PSSNa.

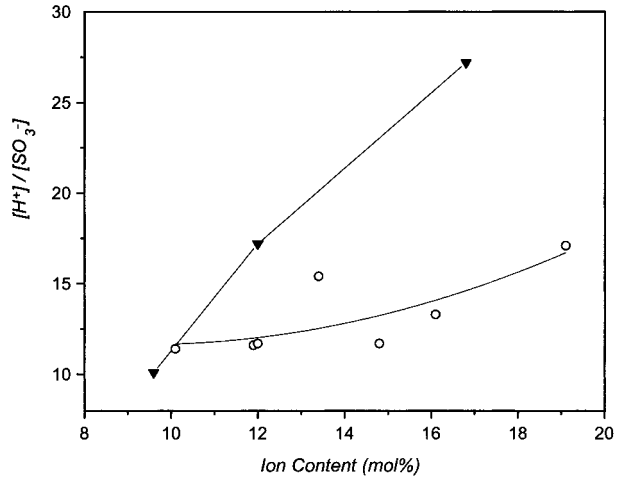

Figure 9. Comparison of water content of PS-*r*-PSSA (triangle) and PS-*g*-*mac*PSSA (circle) copolymer membranes as a function of ion content.

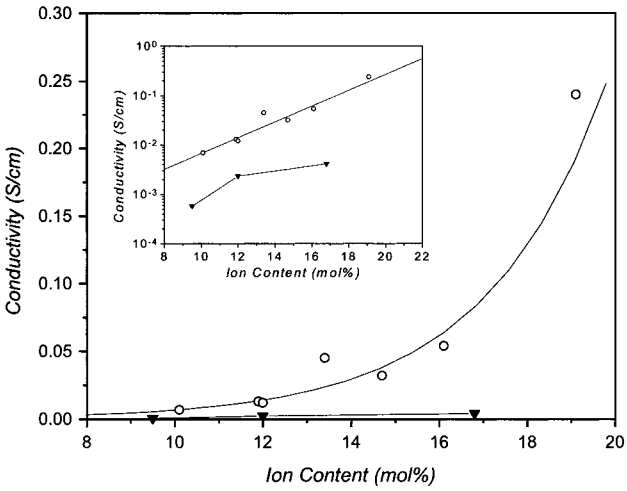

Figure 10. Comparison of proton conductivity of PS-*r*-PSSA (triangle) and PS-*g*-*mac*PSSA (circle) copolymer membranes as a function of ion content. Inset: log scale plot.

the dependence of the copolymer composition on the feed composition was calculated (Figure 2). The measured PSSNa content in the copolymers is lower than expected in all cases because a percentage of PSSNa is removed during washing with water. Furthermore, the conversion of *mac*PSSNa to final product is low (Table 1). This may be because initiation takes place in solution or because a significant fraction of *mac*PSSNa resides in the aqueous phase. When the *mac*PSSNa/styrene feed ratio is low, the incorporation of styrene into the graft polymer is also low. This most likely results from formation of polymer that contains a disproportionately higher percentage polystyrene, which is subsequently removed (dissolved) during washing with THF.

3. Composition and Equivalent Weight. Figure 3 compares the infrared spectra of PS and PSSNa homopolymers with a graft polymer (PS-*g*-*mac*PSSNa) containing 10.1 mol % SSNa (G10). The peak at 1010 cm^{-1} is assigned to in-plane bending of the para-substituted benzene ring, normally observed at 1013 cm^{-1} in completely dry samples.[41,42] The sharp peak at 1040 cm^{-1} is assigned to symmetric stretching of SO_3^-. The broad band around 1181 cm^{-1} is due to antisymmetric stretching of SO_3^-; this band broadens when hydrated, and a shoulder appears at ~1210 cm^{-1}. All three peaks are very sensitive to hydration, as shown below. Peaks at 1453 and 1493 cm^{-1} are both attributed to stretching vibrations of the unsubstituted phenyl ring. Substitution at the para position weakens the peak at 1453 cm^{-1} and shifts the peak at 1493 cm^{-1} to higher frequency.[43] Both peaks are very weak in the spectrum of PSSNa homopolymer. The absorbances at 1453 and 1010 cm^{-1} were therefore used as characteristic peaks for PS and *mac*PSSNa, respectively.

At 1453 cm^{-1} the absorbance is due to both PS and PSSNa such that the absorbance is given by

$$A_{1453} = \epsilon_1 l C_S + \epsilon_2 l C_{SS} \tag{2}$$

where ϵ is the extinction coefficient for the characteristic frequency, l is the thickness of the sample, and C_S and C_{SS} are the molar concentration of PS and PSSNa in the sample, respectively. At 1010 cm^{-1} the contribution to absorbance comes only from PSSNa:

$$A_{1010} = \epsilon_3 l C_{SS} \tag{3}$$

Thus, the ratio of absorbances at 1453 and 1010 cm^{-1} is given by eq 4, where $k_1 = \epsilon_1/\epsilon_3$ and $k_2 = \epsilon_2/\epsilon_3$.

$$A_{1453}/A_{1010} = k_1 C_S/C_{SS} + k_2 \tag{4}$$

By definition, equivalent weight (EW) can be written as a function of C_S/C_{SS} as shown below, where M_{SS} and M_S are the molar masses of sodium styrenesulfonate and styrene, respectively.

$$\mathrm{EW} = M_{SS} + M_S(C_S/C_{SS}) \tag{5}$$

The relationship between A_{1453}/A_{1010} and C_S/C_{SS} shown eq 6 can therefore be established, where $K_1 = k_1/M_S$ and $K_2 = k_2 - k_1(M_{SS}/M_S)$.

$$A_{1453}/A_{1010} = K_1(\mathrm{EW}) + K_2 \tag{6}$$

IR data of a series of graft copolymer samples were calibrated with the molar percentage of sulfonate in the copolymer determined by element analysis. A calibration plot is shown in Figure 4. Equation 6 was fit to the experimental data, from which $K_1 = 0.001\,64$ and $K_2 = -0.236$ (correlation coefficient 0.996). EW data of both graft and random copolymers measured by IR are summarized in Table 2.

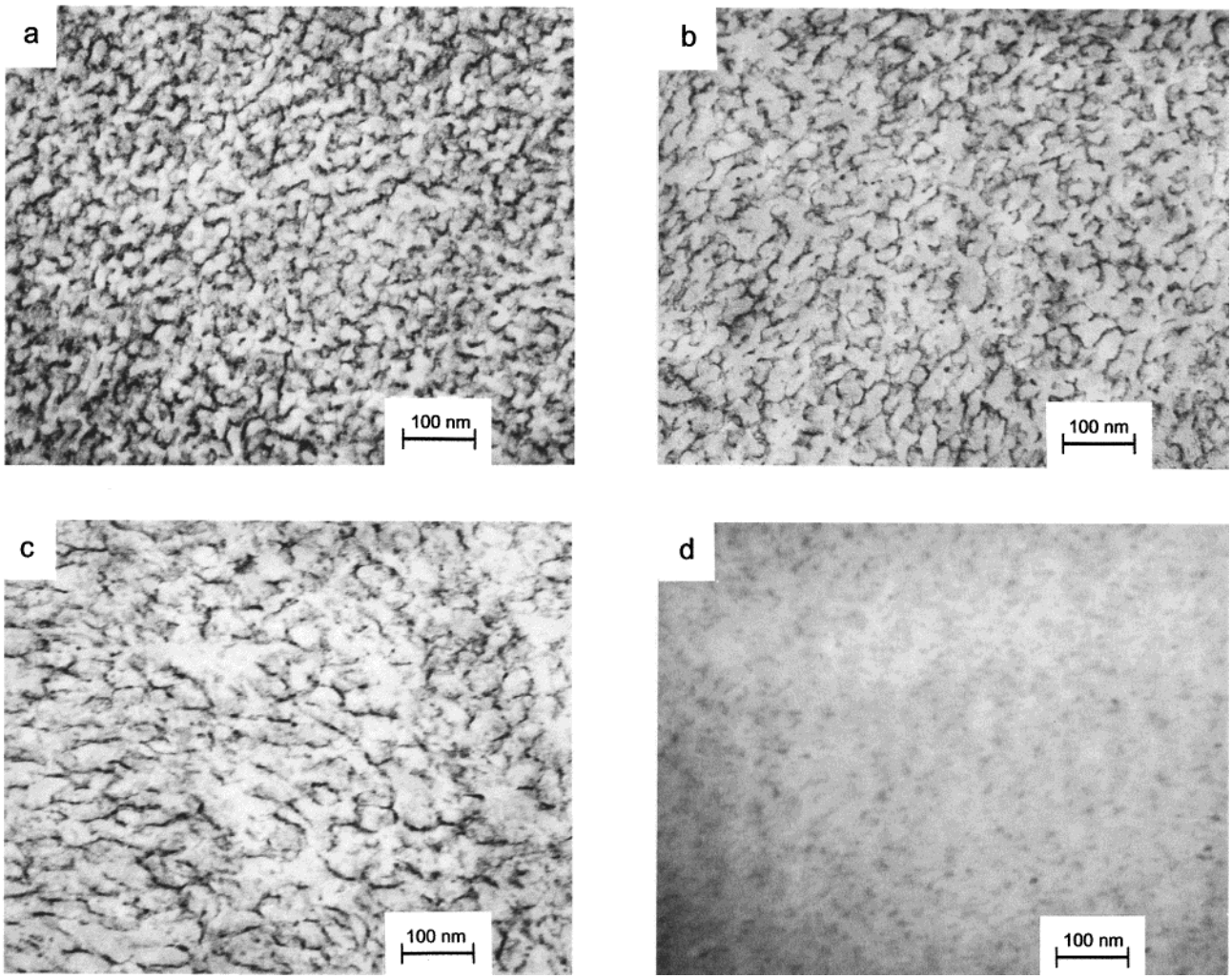

Figure 11. TEM micrographs of Pb^{2+}-stained PS-*g*-*mac*PSSA graft polymer membranes possessing ion contents: 19.1 mol % (a), 11.9 mol % (b), and 8.1 mol % (c) and of a random copolymer membrane (PS-*r*-PSSA), ion content 12.0 mol % (d).

Since the IR peak at 1010 cm^{-1} is sensitive to hydration, caution must be taken in using IR data to determine composition. The ratio A_{1453}/A_{1010} was found to change with time upon exposure of dry samples to ambient air due to the absorption of moisture. Figure 5 shows this effect for a graft polymer film possessing a SSNa content of 16.1% (sample G16). The film was first completely dried by heating to 170 °C under reduced pressure (1 mmHg) for 6 h. FTIR spectra were subsequently recorded in air having a relative humidity of ~25%. The ratio A_{1453}/A_{1010} decreases rapidly (~10%) within a few minutes but reaches equilibrium within 10 min. All IR measurements used for calculations of ion content, and EW were therefore carried out under equilibrium conditions.

In contrast to the traditional back-titration method,[44] membranes were titrated directly in solution. Titration values depend on the ion content of the membrane and the accessibility of individual ionic sites. Figure 6 compares the values of EW determined by IR analysis with that obtained by titration. EW values are in excellent agreement for all graft polymers indicating that all ions in the membrane are accessible. In contrast, the titration method overestimates EW of the random copolymers by up to ~10%, indicating a fraction of sulfonate sites are inaccessible to aqueous solution.

4. Thermal Behavior. Figure 7 compares representative DSC curves for a graft polymer, random copolymer, and polystyrene homopolymer. For all samples, only one transition is observed between 40 and 300 °C. T_g of graft polymers, shown in Table 2, consistently occurs at a higher temperature than PS (101 °C), indicating PS chain motion in the graft polymer is restricted due to the presence of ionic side chains. According to the EHM model,[18] PS chains can be found both in domains of PS and ionic clusters. Similarly, PS domains can contain low concentrations of ion pairs that effectively raise the T_g of the PS domain. This is observed in the graft polymers although the ionic content of the graft copolymer increases and T_g decreases. The latter is qualitative evidence that the degree of phase separation between PS and *mac*PSSNa ionic domains increases with ion content.

The difference in heat capacity associated with the glass transition, ΔC_p (J g^{-1} K^{-1}) was determined. These values are reported in Table 2. ΔC_p decreases with increasing ion content since this transition is primarily associated with the PS domain. More detailed information can be extracted when ΔC_p is normalized to the weight fraction, w_s, of styrene in the polymer. Values of $\Delta C_p/w_s$ for graft and random copolymers are plotted in Figure 8 as a function of ion content and are found to be much lower (0.09−0.20 J/(g K)) than pure PS (0.32 J/(g K)).[45] This indicates that a percentage of styrene units in the copolymer do not undergo a glass transition, presumably because they are associated with ionic

clusters and their correlated motion is restricted. This effect is more pronounced with increasing ion content, which implies that the PS domain size also decreases.

Values of $\Delta C_p/w_s$ for random copolymers are lower than those of the graft polymers, indicating that even fewer polystyrene units undergo a glass transition. These values are similar to those found for previously reported randomly sulfonated polystyrene.[46] Furthermore, T_g of PS-*r*-PSSNa occurs at a higher temperature than PS-*g*-*mac*PSSNa polymers, indicating that the former a less phase separated than the latter.

5. Water Uptake, Proton Conductivity, and TEM. Following the exchange of Na^+ with H^+, membranes were equilibrated in deionized water, and their water content was determined. Data, reported in Table 2, are expressed in terms of water content ($vol_{water}/vol_{wet\ membrane}$) and molar ratio of water to sulfonic acid groups ($[H_2O]/[SO_3^-]$). Figure 9 plots $[H_2O]/[SO_3^-]$ for graft and random copolymers. $[H_2O]/[SO_3^-]$ for PS-*g*-macPSSNa increases incrementally ($\sim 12 \rightarrow 17$) as a function of ion content. The relatively low value of $[H_2O]/[SO_3^-]$ indicates that the elastic forces in the solid polymer offset the considerably large osmotic pressure. In contrast, the $[H_2O]/[SO_3^-]$ ratio increases more substantially for the random copolymers over a similar range of ion content, which indicates that the cohesive hydrophobic interactions are much weaker.

Figure 10 compares the proton conductivity of PS-*g*-*mac*PSSA and PS-*r*-PSSA membranes as a function of ion content. A linear relationship between log σ and percent sulfonic acid is observed for the graft copolymers. The much higher conductivity exhibited by the graft copolymers is striking. Comparison of the graft and random copolymers possessing ~16.1 and 16.8 mol % of sulfonic acid, respectively, indicates the conductivity of the former is 13 times higher even though its water content is 60% lower. The graft polymers with the highest ion content exhibited a conductivity (0.24 S/cm) that is 3−5 times larger than Nafion 117, even though the volume water contents are similar (37 vol % for the graft polymer and 34 vol % for Nafion).[15,21]

TEM analysis was performed on Pb^{2+}-stained PS-*g*-*mac*PSSA and PS-*r*-PSSA membranes. Four micrographs are shown in Figure 11 that compare morphologies of graft and random copolymers with different ion content. The dark regions represent localized ionic domains; the lighter regions represent hydrophobic PS domains. The micrographs provide direct evidence of a biphasic morphology for the graft polymers. The ionic aggregates are visibly connected to yield a continuous ionic network. The density of the ionic pathways increases with ionic content as evidenced from Figure 11a−c and explains why the ionic conductivity rises to relatively high values. While it should be recognized that these micrographs represent "dry" membranes, it is expected that phase separation, and connectivity of ionic/hydrophilic domains will be even more pronounced in water-swollen membranes.

Conclusions

These studies, based on well-defined PS-*g*-*mac*PSSA polymers with a graft chain length of 32 sodium styrenesulfonic acid units, clearly illustrates the importance of phase separation on water sorption and ionic conductivity. The effect of incorporating ionic components as graft chains, as opposed to being dispersed randomly along the main chain, has a strong bearing on water uptake and proton conductivity of resultant membranes. For graft polymers, ionic conductivity can be exceptionally large even though their water contents are relatively low.

While it is recognized that the stability of hydrocarbon-based PEMs are inferior to perfluorinated materials such as Nafion, the information contained in this report provides insight into the role of morphology on PEMs. For example, blocks of ionic components in amphiphilic ionic polymers facilitate phase separation and, if their concentration is sufficiently high, formation of ionic networks. This concept should apply not only to styrene-based polymers but also to more stable proton conducting polymers such as polysulfonated aromatics and polybenzimidazoles. The challenge here is to devise synthetic methodology to achieve block or graft structures. In the case of styrenics, it may be possible to apply the SFRP macromonomer approach to fluorinated and other substituted styrenic analogues, thus increasing their environmental stability. Finally, these concepts should be recognized as being valuable not only in the design of PEMs but also in the design of ion-conducting membranes for battery applications, electrosynthesis, and water purification.

Acknowledgment. This work was financially supported by the Natural Sciences and Engineering Research Council of Canada, Ballard Power Systems Inc., and British Gas Holdings (Canada) Ltd. We thank Dr. D. Bazett-Jones for access to the Electron Microscopy Laboratory, University of Calgary.

References and Notes

(1) Appleby, A. J.; Foulkes, R. L. *Fuel Cell Handbook*; Van Nostrand: New York, 1989.
(2) Niedrach, L. W.; Grubb, W. T. In *Fuel Cells*; Academic Press: New York, 1963; p 259.
(3) Wei, J.; Stone, C.; Steck, A. E. US Patent 5,422,411, 1995.
(4) Steck, A. E.; Stone, C. In *Proceedings of the Second International Symposium on New Materials for Fuel Cell and Modern Battery System*; Savadogo, O., Roberge, P., Eds.; Montreal, 1997; p 792.
(5) Rouilly, M. V.; Koetz, E. R.; Haas, O.; Scherer, G. G.; Chapiro, A. *J. Membr. Sci.* **1993**, *81*, 89.
(6) Scherer, G. G.; Buchi, F. N.; Gupta, B. *Polym. Mater. Sci. Eng.* **1993**, *68*, 114.
(7) Holmberg, S.; Lehtinen; Näsman, J.; Ostrovskii, D.; Paronen, M.; Serimaa, R.; Sundholm, F.; Sundholm, G.; Torell, L.; Torkkeli, M. *J. Mater. Sci.* **1996**, *6*, 1309.
(8) Helmer-Metzmann, F.; Osan, F.; Schneller, A.; Ritter, H.; Ledjeff, K.; Nolte, R.; Thornwirth, R. European Patent 0574791 A2, 1993.
(9) Wainright, J. S.; Wang, J. T.; Wang, D.; Savinell, R. F.; Litt, M. *J. Electrochem. Soc.* **1995**, *142*, L121.
(10) Samms, S. R.; Wasmus, S.; Savinell, R. F. *J. Electrochem. Soc.* **1996**, *143*, 1225.
(11) Kerres, J.; Cui, W.; Junginger, M. *J. Membr. Sci.* **1998**, *139*, 227.
(12) Baldauf, M.; Gebhardt, U.; Preidel, W.; Kerres, J.; Ullrich, A.; Eigenberger, G. *Extended Abstracts of the Third International Symposium on New Materials for Electrochemical Systems*; Montreal, 1999; p 233.
(13) Cornet, N.; Diat, O.; Gebel, G.; Jousse, F.; Marsacq, D.; Mercier, R.; Pineri, M. *Extended Abstracts of the Third International Symposium on New Materials for Electrochemical Systems*; Savadogo, O., Ed.; Montreal, 1999; p 241.
(14) Ehrenberg, S. G.; Serpico, J.; Wnek, G. E.; Rider, J. N. US Patent 5,468,574A, 1995.
(15) Savadogo, O. *J. New. Mater. Electrochem. Syst.* **1998**, *1*, 47.
(16) Rikukawa, M.; Sanui, K. *Prog. Polym. Sci.* **2000**, *25*, 1463.
(17) Inzelt, G.; Pineri, M.; Schultze, J. W.; Vorotyntsev, M. A. *Electrochim. Acta* **2000**, *45*, 2403.
(18) Eisenberg, A.; Hird, B.; Moore, R. B. *Macromolecules* **1990**, *23*, 4098.

(19) Kim, J.-S.; Eisenberg, A. In *Ionomers: Characterization, Theory and Applications*; CRC Press: New York, 1996; p 7.
(20) Eisenberg, A. *Macromolecules* **1970**, *3*, 147.
(21) Sumner, J. J.; Creager, S. E.; Ma, J. J.; DesMarteau, D. D. *J. Electrochem. Soc.* **1998**, *145*, 107.
(22) Wakizoe, M.; Velev, O. A.; Srinivasan, S. *Electrochim. Acta* **1995**, *40*, 335.
(23) Gronowski, A. A.; Jiang, M.; Yeager, H. L.; Wu, G.; Eisenberg, A. *J. Membr. Sci.* **1993**, *82*, 83.
(24) Gierke, T. D.; Munn, G. E.; Wilson, F. C. *J. Polym. Sci., Polym. Phys. Ed.* **1981**, *19*, 1687.
(25) Porat, Z.; Fryer, J. R.; Huxham, M.; Rubinstein, I. *J. Phys. Chem.* **1995**, *99*, 4667.
(26) Hsu, W. Y.; Gierke, T. D. *Macromolecules* **1982**, *15*, 101.
(27) Litt, M. H. *Polym. Prepr. (Am. Chem. Soc., Div. Polym. Chem.)* **1997**, *38*, 80.
(28) Kreuer, K. D. *J. Membr. Sci.* **2001**, *185*, 29.
(29) Ding, J.; Chuy, C.; Holdcroft, S. *Chem. Mater.* **2001**, *13*, 2231.
(30) Keoshkerian, B.; Georges, M. K.; Boils-Boissier, D. *Polym. Prepr. (Am. Chem. Soc., Div. Polym. Chem.)* **1994**, *35*, 797.
(31) Keoshkerian, B.; Georges, M. K.; Boils-Boissier, D. *Macromolecules* **1995**, *28*, 6381.
(32) Bouix, M.; Gouzi, J.; Charleux, B.; Vairon, J. P.; Guinot, P. *Macromol. Rapid Commun.* **1998**, *19*, 209.
(33) Hawker, C. J. *Acc. Chem. Res.* **1997**, *30*, 373.
(34) Weiss, R. A.; Turner, S. R.; Lundberg, R. D. *J. Polym. Sci., Polym. Chem. Ed.* **1985**, *23*, 525.
(35) Turner, S. R.; Weiss, R. A.; Lundberg, R. D. *J. Polym. Sci., Polym. Chem. Ed.* **2000**, *23*, 535.
(36) Seop, H.; Demoen, P. J. A. *Microchem. J.* **1960**, *4*, 77.
(37) Gardner, C. L.; Anantaraman, A. V. *J. Electroanal. Chem.* **1995**, *395*, 67.
(38) Anantaraman, A. V.; Gardner, C. L. *J. Electroanal. Chem.* **1996**, *414*, 116.
(39) Kazmaier, P. M.; Daimon, K.; Georges, M. K.; Hamer, G. K. *Polym. Prepr. (Am. Chem. Soc., Div. Polym. Chem.)* **1996**, *37*, 485.
(40) Barclay, G. G.; Hawker, C. J.; Ito, H.; Orellana, A.; Malefant, P. R. L.; Sinta, R. F. *Macromolecules* **1998**, *31*, 1024.
(41) Colthup, N. B.; Daly, L. H.; Wiberley, S. E. *Introduction to Infrared and Raman Spectroscopy*; Academic Press: Boston, 1990.
(42) Fitzgerald, J. J.; Weiss, R. A. *Coulombic Interaction in Macromolecular Systems*; ACS Symposium Series; American Chemical Society: Washington, DC, 1986; Vol. 302, p 35.
(43) Avram, M.; Mateescu, G. D. *Infrared Spectroscopy, Application in Organic Chemistry*; Wiley-Interscience: New York, 1972; p 212.
(44) Barnes, D. J. In *Ionomers: Characterization, Theory and Application*; Schlick, S., Ed.; CRC Press: New York, 1996; p 114.
(45) Ichihara, S.; Komatsu, A.; Tsujita, Y.; Nose, T.; Hata, T. *Polym. J.* **1971**, *2*, 530.
(46) Yang, S.; Sun, K.; Risen, W. M., Jr. *J. Polym. Sci., Part B: Polym. Phys.* **1990**, *28*, 1685.

MA010970M